Solid Freeform Fabrication 2022: Proceedings of the 33rd Annual International Solid Freeform Fabrication Symposium – An Additive Manufacturing Conference
Reviewed Paper

Additively Manufactured 316L Stainless Steel: Effect of Heat Treatment on Microstructure and Tensile Properties

Seungjong Lee[1,2], Reza Ghiaasiaan[1,2], Shuai Shao[1,2], Paul R. Gradl[3], Nima Shamsaei[1,2*]

[1] Department of Mechanical Engineering, Auburn University, Auburn, AL 36849, USA

[2] National Center for Additive Manufacturing Excellence (NCAME), Auburn University, Auburn, AL 36849, USA

[3] NASA Marshall Space Flight Center, Propulsion Department, Huntsville, AL 35812, USA

[*]Corresponding author:
Email: shamsaei@auburn.edu
Phone: (334) 844 4839

Abstract

The microstructure and tensile properties of 316L stainless steel (SS) fabricated using the laser powder directed energy deposition (LP-DED) after various heat treatment (HT) steps such as stress-relief (SR), solution annealing (SA), and hot isostatic pressing (HIP) are characterized. Microstructures before and after HTs are analyzed using both optical and scanning electron microscopy (SEM). Both quasi-static uniaxial tensile and hardness tests are performed to measure mechanical properties. The tensile results indicate that the non-heat treated (NHT) condition possesses higher strengths but lower ductility as compared to the other HT conditions (i.e., SR, SA, HIP, SR+SA, and SR+HIP). By employing the two-step HT conditions (i.e., SR+SA and SR+HIP), no significant changes on tensile properties as compared to the individual single-step HT conditions (i.e., SA or HIP) are observed. The findings suggest that two-step HTs are not required for LP-DED 316L SS unless HIP is needed to minimize volumetric defect contents.

Keywords: 316L stainless steel; Laser powder directed energy deposition; Heat treatment; Microstructure; Tensile properties

Introduction

LP-DED is an additive manufacturing (AM) method that uses injected metal powder flow as feedstocks and the laser beam as an energy source to deposit the powder materials layer by layer to obtain the near net-shaped components [1]. The LP-DED technique has some benefits compared to other AM methods such as fabrication of relatively larger parts, repair capabilities of damaged or faulty components, the ability to clad different materials on existing parts , and reduced material waste [1][2].

Austenite SS such as 304L SS and 316L SS is commonly used SS in numerous industrial applications due to their great corrosion resistance, oxidation resistance, and formability [3,4]. Recently, they have received a lot of attention from AM community. Many researchers have investigated the effects of processing parameters including laser power, scan speed, and hatching distance on microstructure and mechanical properties [5,6]. Even with optimized process parameters, the AM 316L SS has shown anisotropic mechanical properties and corrosion resistance which could be attributed to the characteristic thermal history experienced during AM

fabrication processes which accordingly could affect the alloy's microstructure [7]. One common way used in the community to reduce the anisotropic properties in AM components is post-process HT [8][9]. However, due to the AM's unique thermal history, the standard HTs may or may not achieve similar effects on microstructures and mechanical properties of the AM alloys as they do on conventionally processed counterparts.

Two-step or multi-step HTs become common practices for AM components to resolve anisotropic properties due to mainly rapid cooling in AM process. The SR is considered a first step for the AM parts to remove the residual stresses induced during fabrication processes. SR is usually conducted before removing the parts from the build plate. After SR, conventionally standardized HTs such as annealing and aging for wrought materials are also utilized in AM materials to homogenize and enhance microstructures and mechanical properties, respectively. Furthermore, the HIP process is frequently used for AM materials since it has been proved to be beneficial effect on closing up certain types of defects induced during AM fabrication processes [10].

This study examines the effect of such two-step HTs on 316L SS fabricated by LP-DED technology. Three different two-step HTs such as SR at 899°C + standard SA, SR at 1010°C + standard SA, and SR at 899°C + standard HIP were considered. All three two-step HTs were further compared with single-step HTs (i.e., SR at 899°C, standard SA, or standard HIP). The effects of HTs were studied on microstructure as well as on uniaxial tensile behaviors of the alloy. This article is presented in the following sequences. First, the experimental procedures such as materials preparation and testing are explained. Then, the experimental results are presented and discussed; and finally, conclusions are drawn.

Experimental Procedure

The gas atomized virgin 316L SS powders used to fabricate specimens were provided by the Carpenter Additive. **Table 1** lists the chemical composition of the 316L SS powders along with the nominal composition of the alloy according to ASTM A240/UNS standard [11]. LP-DED 316L SS cylindrical rods (15.24 mm Dia. × 104.14 mm height) were fabricated vertically (i.e., parallel to loading direction) using the following parameters: laser power of 1070 W, layer height of 381 µm, travel speed of 1016 mm/min, and powder feed rate of 15.20 g/min.

Table 1 The chemical composition of 316L SS powder used in this study along with the nominal composition of the alloy according to ASTM standard A240/UNS [11].

	Nominal (ASTM A240/UNS)		Measured
	Min	**Max**	
Fe	Balance		65.80
Cr	16.0	18.0	17.73
Ni	10.0	14.0	12.70
Mo	2.00	3.00	2.41
Mn		< 2.00	0.58
Si		< 0.75	0.62
N		< 0.10	0.10

C		< 0.030	0.02
P		< 0.045	0.007
S		< 0.030	0.006

The cylindrical rods were heat treated using various HT schedules as listed in **Table 2**. Different variables used for the HTs in this study such as temperatures and soaking times of SR and HIP were designed according to the standard AMS 2759 [12] and ASTM F3301 [10] procedures. In addition, extra coupons (15.24 mm Dia. × 3 mm thickness) were heat treated separately for further investigation to examine the effects of holding temperatures ranging from 600°C to 1200°C on microstructures.

Table 2 Details of different heat treatment recipes.

Heat treatments	SR	SA	HIP
NHT	-	-	-
HT01	899°C / 2 hours / Air cooling	-	-
HT02	-	1100°C / 2 hours / Argon quenching	-
HT03	899°C / 2 hours / Air cooling	1100°C / 2 hours / Argon quenching	-
HT04	1010°C / 2 hours / Air cooling	1100°C / 2 hours / Argon quenching	-
HT05	-	-	1163°C / 3 hours / 103 MPa / Argon quenching
HT06	899°C / 2 hours / Air cooling	-	1163°C / 3 hours / 103 MPa / Argon quenching

According to ASTM E3 [13], small coupons from specimens listed in **Table 2** and extra coupons were prepared for the standard metallographic characterization. Microstructures of all HTs were analyzed by KEYENCE VHX-6000X optical microscope and Zeiss Crossbeam 550 scanning electron microscope (SEM) equipped with electron backscatter diffraction (EBSD) and elemental diffraction spectroscopy (EDS) detectors. The microstructural analysis was performed on both normal and transverse planes (i.e., perpendicular and parallel to the build orientation, respectively) for all HT coupons. For optical microscopy, heat treated small coupons were chemically etched using HCL:HNO_3:CH_3COOH etchant to reveal microstructure and meltpool [14]. EBSD scans were conducted using followed configurations: magnification of 50X, voltage of 15 kV, current of 200 pA, and step size of 4µm. The average grain sizes and annealing twins were measured from the EBSD data. It should be noted that the average grain sizes were calculated excluding the $\sum 3$ twin boundaries to avoid miscalculation of twins as grains.

Upon HTs, cylindrical rods were machined to the final geometry of tensile test specimens specified the ASTM E8 standard [15], as shown in **Figure 1**. Uniaxial tensile tests were conducted on test specimens with HTs listed in the **Table 2** using a strain rate of 0.001 mm/mm/s according

to the ASTM E8 standard procedure [15]. An extensometer was used during the initial stage of tensile tests until a 0.045 mm/mm strain for accurate determination of yield strength. Upon removal of the extensometer, the tests were resumed using the displacement-controlled mode. The average values reported for the tensile properties, i.e., the average ultimate tensile strength (UTS), yield strength (YS), and elongation to failure (EL), were calculated over two test data.

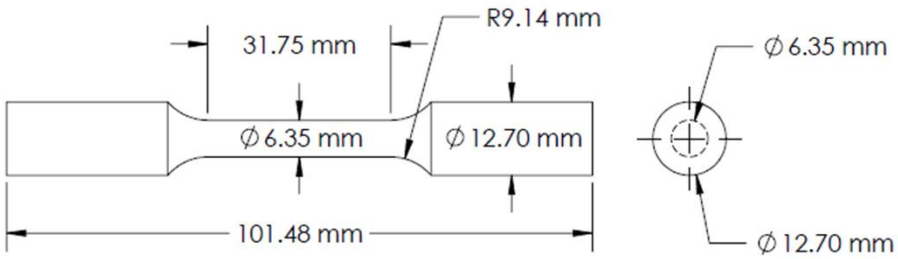

Figure 1 Geometry of tensile test specimens according to ASTM E8 [15].

Results and Discussion

The microstructures of NHT and HT coupons were analyzed by optical microscopy and are presented in **Figure 2** and **Figure 3**, respectively. The melt pool boundaries and fine dendritic microstructures, which are the characteristics of the AM materials [14], are visible in the normal and transverse planes of NHT specimens. As shown, the melt pool boundaries and dendritic microstructures have not been fully removed until 900 °C. The coupons heat treated by temperatures above 1000 °C do not present melt pool boundaries and fine dendritic microstructures anymore. It indicates that some recrystallization and grain growth has occurred.

The inverse pole figures (IPF) and grain boundaries obtained from EBSD analysis are shown in **Figure 4** for all HTs. As shown, increasing the temperature of the first step of HTs up to 1000°C does not show significant effects on average grain sizes. In addition, the number of annealing twins that are calculated using the percentage of $\sum 3$ coincidence site lattice (CSL) boundaries is not changed by HTs using temperatures below 1000°C. Similar observations were reported from wrought 316L SS counterparts in the literature [16]. The average grain size and annealing twin fraction are increased when the HT temperatures are higher than 1000°C. It again suggests that recrystallization and grain growth have been caused.

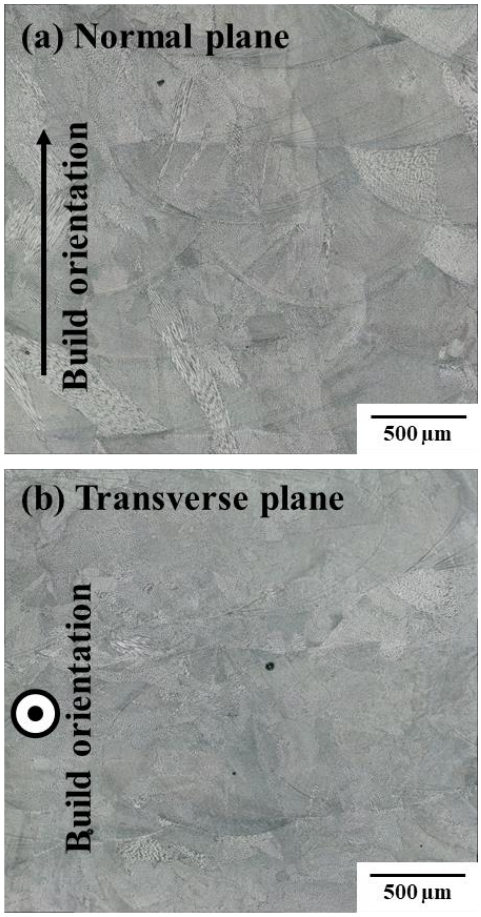

Figure 2 Optical micrographs of LP-DED 316L SS in NHT condition obtained on normal plane in (a) and transverse plane in (b) (i.e., parallel and perpendicular to the build orientation, respectively).

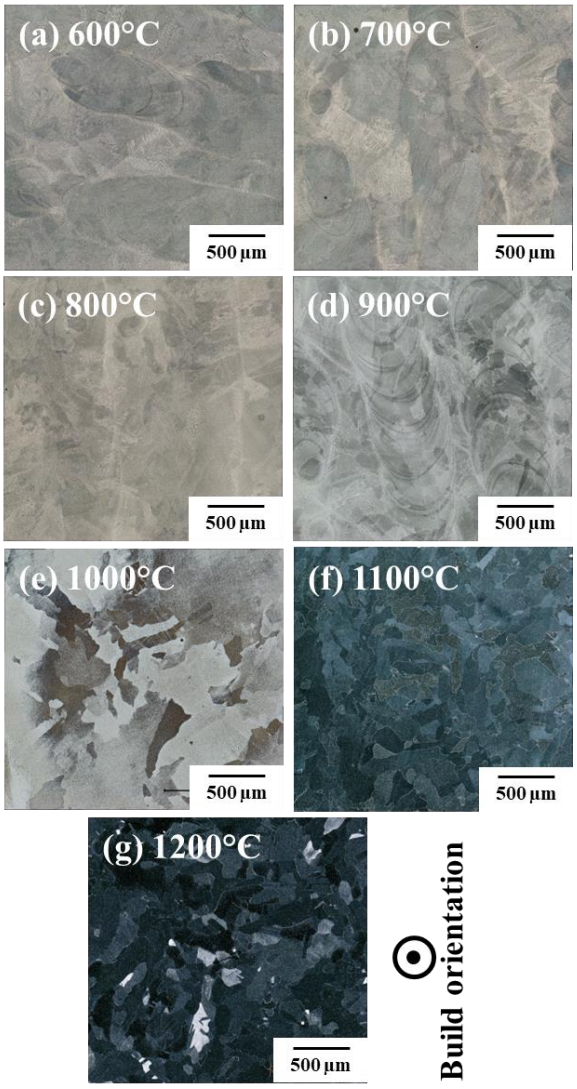

Figure 3 Optical micrographs of LP-DED 316L SS heat treated by holding temperatures of (a) 600°C, (b) 700°C, (c) 800°C, (d) 900°C, (e) 1000°C, (f) 1100°C, and (g) 1200°C for 2 hours.

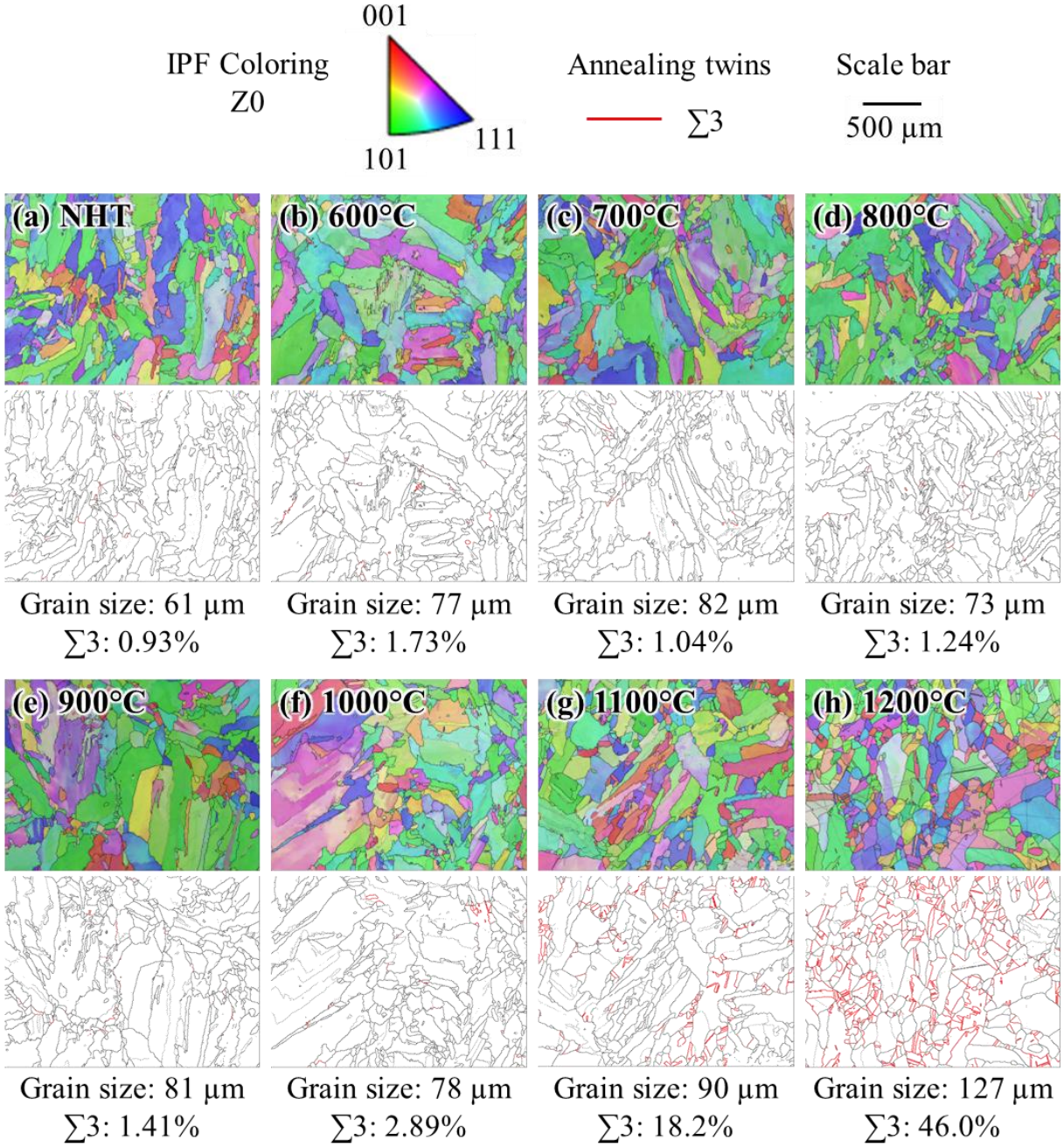

Figure 4 Inverse pole figure (IPF) and grain boundaries of specimens after heat treated by different temperatures: (a) NHT, (b) 600°C, (c) 700°C, (d) 800°C, (e) 900°C, (f) 1000°C, (g) 1100°C, and (h) 1200°C.

The tensile results, including the stress-displacement curves, and bar graphs of all specimens are presented in **Figure 5**. Furthermore, the details of tensile properties such as the ultimate tensile strength (UTS), yield strength (YS), and elongation to failure (EL) of each condition are listed **Table 3**. As shown in **Figure 5** and **Table 3**, the NHT specimen has shown the highest UTS of 581.09 MPa and YS of 398.65 MPa and the relatively low EL of 81.25%. Tensile properties LP-DED 316L SS fall the mechanical test requirements proposed by ASTM A240 standard of the wrought 316L SS counterparts that are presented as dotted lines in **Figure**

5(b) [11]. However, UTS and YS are lower than the laser beam powder bed fusion (L-PBF) 316L SS (UTS of 612 MPa and YS of 490 MPa) regardless of HT conditions [8].

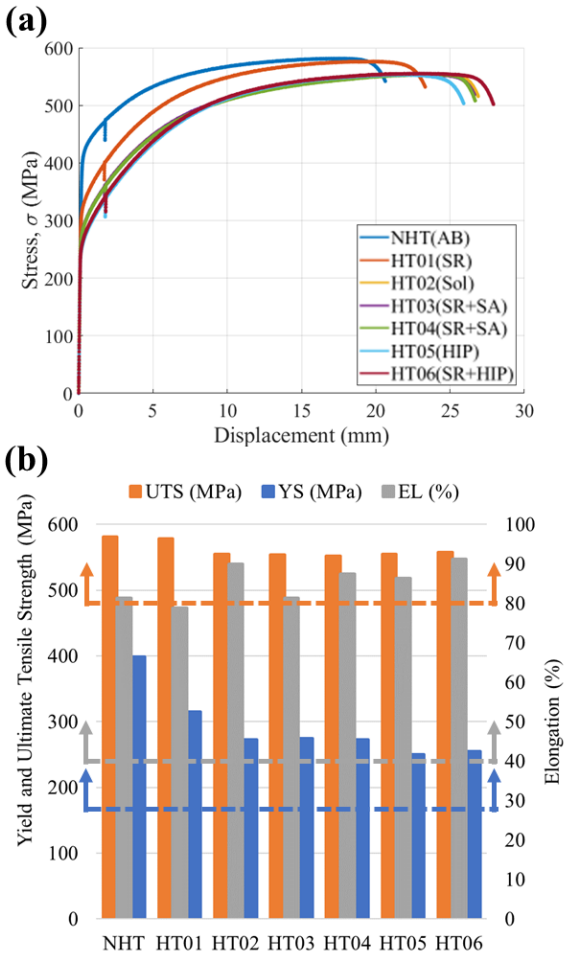

Figure 5 Uniaxial tensile behavior of LP-DED 316L SS specimens in NHT and different HT conditions: (a) stress-displacement curves and (b) bar chart of UTS, YS, and EL for each HT condition. ASTM A240 mechanical test requirements are presented as dotted lines in (b).

Table 3 UTS, YS, and EL of specimens after each heat treatment.

Heat treatment	UTS (MPa)	YS (MPa)	Elongation (%)
NHT (AB)	581.09	398.65	81.25
HT01 (SR)	578.36	314.56	78.75
HT02 (SA)	554.91	272.43	81.25
HT03 (SR+SA)	553.85	274.53	90.00
HT04 (SR+SA)	551.81	272.76	87.50
HT05 (HIP)	554.18	249.86	86.25
HT06 (SR+HIP)	557.48	254.52	91.25

As shown earlier, the SR at 899°C for 2h (HT01) does not have significant effects on the microstructure of LP-DED 316L SS specimens as compared with NHT conditions. It could be

attributed to the low temperature, which subsequently resulted in similar UTS and YS in SR (HT01) as compared to the NHT specimen. Except for the HT01 specimens, all the other HTs have shown similar UTS and YS, which were lower than those of the NHT specimen. As discussed earlier in the previous section, this could be ascribed to the effect of HT temperature during the first step on microstructure, resulting in better homogenization and removal of microsegregation and dendritic microstructures which may have some strengthening effect [17].

As shown in **Figure 5**, the two-step HT conditions such as SR at 899°C/2h + SA (HT03), SR at 1010°C/2h + SA (HT04), and SR at 899°C/2h + HIP (HT06) do not show significant changes on tensile properties as compared to the single-step HT conditions (i.e., SA (HT02) and HIP (HT05)). It implies that standard SA without SR can bring reasonable microstructural homogenizations resulting in insignificant effects on tensile properties. However, HIP is commonly required to reduce volumetric defects of AM material [10]. Therefore, HIP is still important for fatigue critical applications because the volumetric defects can be the major cause of the early fatigue crack initiations resulting in short fatigue lives [18].

Conclusions

In this study, the effects of different heat treatment conditions on microstructure and uniaxial tensile properties of LP-DED 316L SS were investigated. The following conclusions could be drawn on the experimental observations:

- The melt pool boundaries and fine-scale cellular structures were not fully removed when the holding temperature was below 1000 °C, due to the sluggish diffusion.
- Upon HT at higher temperatures than 1000°C, the average grain size and annealing twin fraction increased, suggesting that some recrystallization/grain growth occurred.
- Tensile properties of LP-DED 316L SS in non-heat treated consistent with those of mechanical test requirements dictated by the ASTM A240 standard; they showed slight inferiority as compared to the L-PBF 316L SS.
- Tensile strengths of LP-DED 316L SS in NHT were the highest among all HT conditions which were traded off with the relatively low elongation to failure.

Acknowledgement

This research is partially supported by the National Aeronautics and Space Administration NASA under Cooperative Agreement No. 80MSFC19C0010. This paper describes objective technical results and analysis. Any subjective views or opinions that might be expressed in the paper do not necessarily represent the views of the National Aeronautics and Space Administration (NASA) or the United States Government.

References

[1] Zhang Y, Wu L, Guo X, Kane S, Deng Y, Jung YG, et al. Additive Manufacturing of Metallic Materials: A Review. J Mater Eng Perform 2018;27:1–13. https://doi.org/10.1007/s11665-017-2747-y.

[2] Herderick ED. Accelerating the Additive Revolution. Jom 2017;69:437–8. https://doi.org/10.1007/s11837-017-2262-5.

[3] Chen XH, Lu J, Lu L, Lu K. Tensile properties of a nanocrystalline 316L austenitic stainless steel. Scr Mater 2005;52:1039–44. https://doi.org/10.1016/j.scriptamat.2005.01.023.

[4] Lee S, Pegues J, Shamsaei N. Fatigue Behavior and Modeling for Additive Manufactured

304L Stainless Steel: The effect of Surface Roughness. Int J Fatigue 2020;141:105856. https://doi.org/10.1016/j.ijfatigue.2020.105856.

[5] Suryawanshi J, Prashanth KG, Ramamurty U. Mechanical behavior of selective laser melted 316L stainless steel. Mater Sci Eng A 2017;696:113–21. https://doi.org/10.1016/j.msea.2017.04.058.

[6] De Lima MSF, Sankaré S. Microstructure and mechanical behavior of laser additive manufactured AISI 316 stainless steel stringers. Mater Des 2014;55:526–32. https://doi.org/10.1016/j.matdes.2013.10.016.

[7] Feenstra DR, Cruz V, Gao X, Molotnikov A, Birbilis N. Effect of build height on the properties of large format stainless steel 316L fabricated via directed energy deposition. Addit Manuf 2020;34:101205. https://doi.org/10.1016/j.addma.2020.101205.

[8] Blinn B, Klein M, Gläßner C, Smaga M, Aurich JC, Beck T. An investigation of the microstructure and fatigue behavior of additively manufactured AISI 316L stainless steel with regard to the influence of heat treatment. Metals (Basel) 2018;8. https://doi.org/10.3390/met8040220.

[9] Zhang X, Mcmurtrey MD, Wang L, Brien RCO, Shiau C, Wang YUN, et al. Evolution of Microstructure , Residual Stress , and Tensile Properties of Additively Manufactured Stainless Steel Under Heat Treatments. JOM 2020;72:4167–77. https://doi.org/10.1007/s11837-020-04433-9.

[10] ASTM F3301. Standard for Additive Manufacturing – Post Processing Methods – Standard Specification for Thermal Post-Processing Metal Parts Made Via Powder Bed Fusion. ASTM Stand 2018:3. https://doi.org/10.1520/F3301-18A.2.

[11] American Society for Testing and Materials. ASTM A240: Standard Specification for Chromium and Chromium-Nickel Stainless Steel Plate , Sheet , and Strip for Pressure Vessels and for General Applications. ASTM Int 2004;I:12. https://doi.org/10.1520/A0240.

[12] Committee AMSEC and LAS. Heat Treatment of Steel Parts General Requirements 2019. https://doi.org/https://doi.org/10.4271/AMS2759G UI - AMS2759G.

[13] Interanational A. Standard Guide for Preparation of Metallographic Specimens Standard Guide for Preparation of Metallographic Specimens 1. ASTM Int 2012;03.01:1–12. https://doi.org/10.1520/E0003-11R17.1.

[14] Nezhadfar PD, Shamsaei N, Phan N. Enhancing ductility and fatigue strength of additively manufactured metallic materials by preheating the build platform. Fatigue Fract Eng Mater Struct 2021;44:257–70. https://doi.org/10.1111/ffe.13372.

[15] ASTM International. ASTM E8/E8M standard test methods for tension testing of metallic materials. West Conshohocken, PA 2010:1–27. https://doi.org/10.1520/E0008.

[16] Huang W, Yuan S, Chai L, Jiang L, Liu H, Wang F, et al. Development of Grain Boundary Character Distribution in Medium-Strained 316L Stainless Steel During Annealing. Met Mater Int 2019;25:364–71. https://doi.org/10.1007/s12540-018-0203-7.

[17] Ghiaasiaan R, Muhammad M, Gradl PR, Shao S, Shamsaei N. Superior tensile properties of Hastelloy X enabled by additive manufacturing. Mater Res Lett 2021;9:308–14. https://doi.org/10.1080/21663831.2021.1911870.

[18] Moran TP, Carrion PE, Lee S, Shamsaei N, Phan N, Warner DH. Hot Isostatic Pressing for Fatigue Critical Additively Manufactured Ti-6Al-4V. Materials (Basel) 2022;15:1–12. https://doi.org/10.3390/ma15062051.